Modeling the Sediment Load of the Doce River after the Fundão Tailings Dam Collapse, Brazil

Marcos C. Palu, S.M.ASCE[1]; and Pierre Y. Julien, M.ASCE[2]

Abstract: The collapse of the Fundão tailings dam in Brazil spilled 32 million cubic meters of mine waste, causing a severe socioeconomic and environmental impact in the Doce River. Approximately 90% of the spilled volume settled on floodplains, over 118 km downstream of Fundão Dam. A hyperconcentrated flow (≈400,000 mg/L) reached the Doce River, where the floodwave and sediment wave traveled at different celerities over 570 km until the Atlantic Ocean. The one-dimensional advection-dispersion equation with settling was solved and calibrated to fit the observed concentration using an analytical solution to determine the longitudinal dispersion coefficient and the settling rate, both along the river and in the reservoirs. The longitudinal dispersion coefficient ranged from 30 to 120 m^2/s, and the sediment settling rate corresponded to particle sizes from 1.1 to 2.0 μm. Moreover, simulations with the calibrated model revealed that without the presence of three hydropower reservoirs on the Doce River, the sediment concentration at the watershed outlet would have been 64,000 mg/L instead of the observed 1,500 mg/L. The temperature effects were also examined, and a decrease from 30°C to 5°C in water temperature would have caused a concentration 12 times higher at the outlet. **DOI: 10.1061/(ASCE)HY.1943-7900.0001582.**

Author keywords: Tailings dam collapse; Fundão tailings dam; Transport of suspended sediment; One-dimensional advection-dispersion equation; Longitudinal dispersion coefficient; Sediment settling rate; Doce River.

Introduction

Numerous tailings dam failures around the world have caused extensive environmental and socioeconomic impacts. For mine tailings dams, the consequences may be aggravated by the presence of waste material from mining activities, which can cause irreversible environmental damage downstream (Kossoff et al. 2014). The frequency of such incidents is disturbing. Davies et al. (2000) investigated the occurrence of tailings dams failures over 30 years (1970–1999), counting two to five major failures per year. Davies (2002) also compared the frequency of collapses of tailings dams with water storage dams using the same 30-year database. The author concluded that the rate of tailings dam failure is approximately 10 times higher than that for conventional dams.

In the new millennium, tailings dam accidents around the world occur at an alarming rate (Azam and Li 2010; Caldwell et al. 2015; WISE 2016). To name a few: Kingston Fossil Plant 2008 (Tennessee—United States), Karamkem 2009 (Russia), Huancavelica 2010 (Peru), Mianyang City 2011 (China), Sotkamo 2012 (Finland), Obed Mountain Coal Mine 2013 (Canada), Dan River Steam Station 2014 (North Carolina—United States), Mount Polley 2014 (Canada), Buenavista 2014 (Mexico), Fundão 2015 (Brazil), Hpakant 2015 (Myanmar), New Walles 2016 (Florida—United States), Tonglvshan 2017 (China), and Mishor Rotem 2017 (Israel).

The current state of the art on research about tailings dams failures is mainly focused on the hydrograph generated by the dam break and the related floodwave propagation in the vicinity of the dam. A widespread method for the calculation of reach and velocity of the resultant flood requires the solution of the shallow water equation, adding an additional friction term in order to take into account the resistance due to hyperconcentrated flow characteristics (Jeyapalan et al. 1983; Schamber and MacArthur 1985; O'Brien et al. 1993; Jin and Fread 1999; Rickenmann et al. 2006; Armanini et al. 2009; Kunkel 2011; Lin and Li 2012; Marsooli et al. 2013).

However, it should be highlighted that there are several incidents where mine waste spills have more severe consequences than the dam collapse. The release of substances (often toxic) in river systems contaminates the river sediment and harms aquatic and human life for hundreds of kilometers (Kossoff et al. 2014). The example of the Baia Mare and Baia Borsa tailings dams in Romania comes to mind. The spilled tailings, composed of cyanide, lead, copper, and zinc were released in the River Tisa, a major Danube tributary. This accident resulted in tons of fish deaths in Romania, Hungary, Serbia, and Bulgaria. The flow continued into the Danube River and eventually reached the Black Sea 1,900 km downstream (ICOLD 2001; Kossoff et al. 2014).

In addition, there are spill accidents not involving dam failure, as in the recent case of the Gold King Mine in Colorado (United States), which discharged 11,000 m^3 of acid mine water into the Animas and San Juan Rivers on August 5, 2015.

This accident caused the propagation and deposition of toxic heavy metals along the two affected rivers, until the plume reached Lake Powell in Utah on August 14, 2015 (USBR 2015).

With a focus on accidental mine tailings propagation in a river, the present study describes the development of detailed modeling tools to determine the sediment transport in the Doce River as a consequence of the collapse of the Fundão tailings dam in Brazil, on November 5, 2015. The dam break released 32 million cubic meters of tailings, causing the destruction of the town of Bento Rodrigues, including 19 casualties and extensive socioeconomic and

[1]Ph.D. Candidate, Dept. of Civil and Environmental Engineering, Colorado State Univ., Fort Collins, CO 80523 (corresponding author). ORCID: https://orcid.org/0000-0002-6132-7125. E-mail: marcos.palu@colostate.edu

[2]Professor, Dept. of Civil and Environmental Engineering, Colorado State Univ., Fort Collins, CO 80523. E-mail: pierre@engr.colostate.edu

Note. This manuscript was submitted on April 12, 2018; approved on October 3, 2018; published online on February 21, 2019. Discussion period open until July 21, 2019; separate discussions must be submitted for individual papers. This paper is part of the ***Journal of Hydraulic Engineering***, © ASCE, ISSN 0733-9429.

environmental damage to the Doce River watershed (ANA 2016b). According to Morgenstern et al. (2016), the accident happened at 3:45 p.m. (local time) and was caused by liquefaction and flowsliding of the sand stored in the reservoir. The authors described the employee report just before the accident: "At 3:45 p.m. shouts came over radio that the dam was collapsing. A cloud of dust had formed over the left abutment, and those closest to the area designated the 'setback' could see cracks forming at the recently constructed drainage blanket. The slope above them was beginning to undulate 'like a wave' as if it were 'melting,' bringing the dam crest down after it. The tailings that had looked like solid ground just minutes before transformed into a rolling river."

According to a survey carried out by the Brazilian Institute of Environment and Renewable Natural Resources (IBAMA 2016), approximately 90% of the volume spilled was deposited in the first 118 km downstream of the dam, that is, before the first hydropower plant reservoir in the Doce River (Candonga Dam). The remaining tailings reached the Doce River, causing severe environmental and social impact in the towns around the river.

The floodwave traveled a total distance of 670 km along the Doce River watershed, causing the death of nearly 3 t of fish and the disruption of water supply in 12 cities, affecting an estimated population of 424,000 people (ANA 2016b; IBAMA 2016). This is the all-time worst Brazilian environmental accident (Marta-Almeida et al. 2016; do Carmo et al. 2017).

After the dam break, the Geological Service of Brazil and the National Water Agency conducted several measurements along the Doce River in order to track the impact of the floodwave and the high turbidity (CPRM and ANA 2015). The Brazilian agencies collected data of discharge, water level, temperature, dissolved

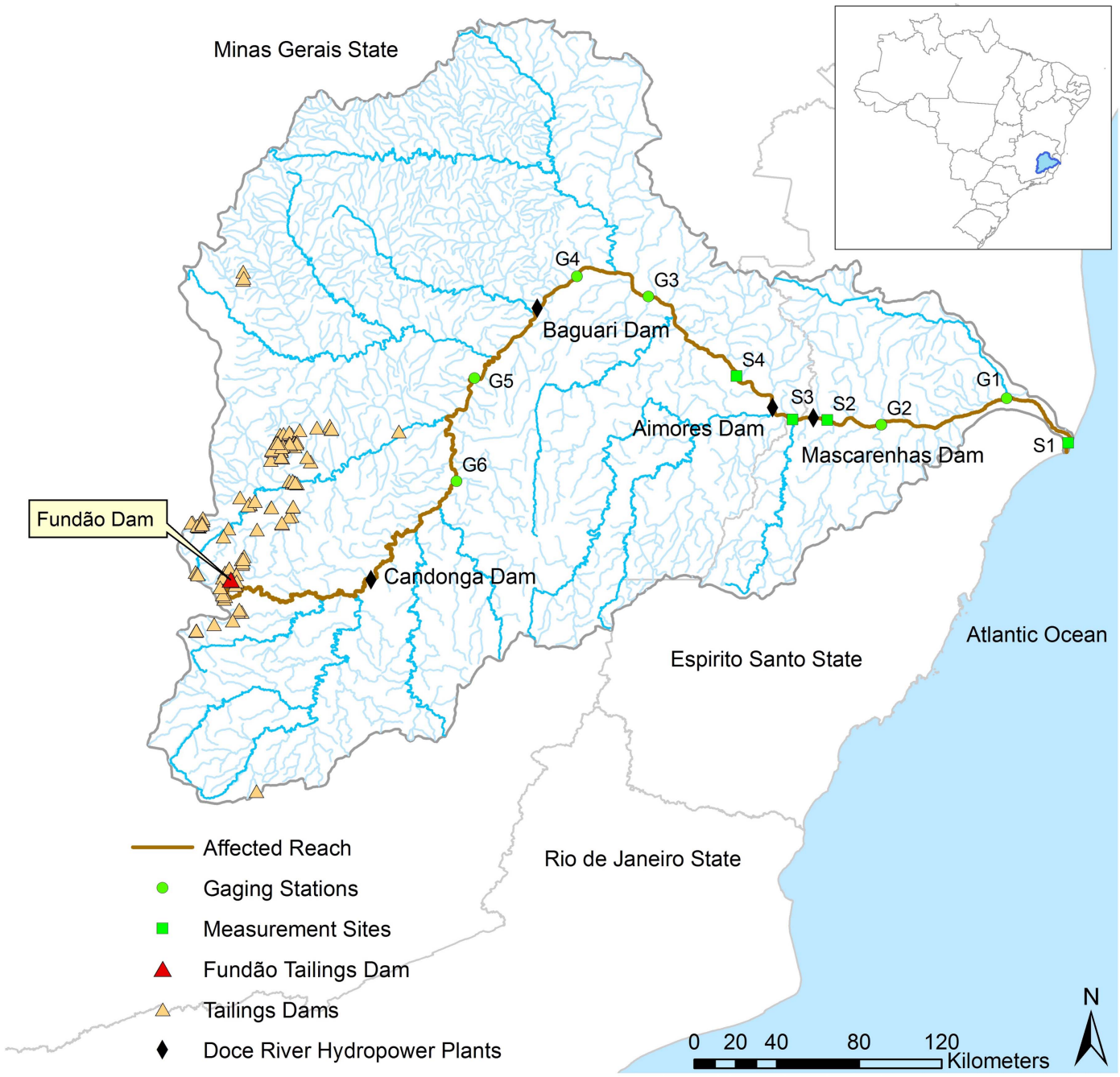

Fig. 1. Doce River watershed: location of the Fundão Dam and gauging stations.

oxygen, pH, turbidity, particle size, and concentration of sediments in suspension. These are valuable data because the availability of measurements after the collapse of a tailings dam is uncommon in the literature (Rico et al. 2008).

Thus, the main objectives of this paper are: (1) to determine the proper equation to model the sediment propagation along the Doce River after the tailings dam collapse, (2) to determine the longitudinal dispersion coefficient and settling rate along the Doce River after the tailings dam collapse, (3) to simulate what the sediment concentration along the Doce River would be without the retention from the hydropower plant reservoirs, and (4) to investigate the effect of the temperature on sediment settling.

Site Description

Doce River Watershed

The Fundão Dam is one of the 106 tailings impoundments located in the Doce River Watershed in the southeast region of Brazil. This watershed has a drainage area of 82,600 km^2, with most of the area located in the state of Minas Gerais (86%), and the remaining in the state of Espirito Santo. The main stream is called the Doce River, comprising an extension of 570 km and flowing then to the Atlantic Ocean. There are 225 towns in the Doce River watershed, which corresponds to a population of approximately 3.6 million inhabitants (ANA 2016b). The Doce River plays a critical role through electric power generation, supporting the local economy and providing essential water for domestic, agricultural, and industrial uses.

The Fundão Dam was a 120-m high tailings dam, containing approximately 56 million cubic meters of tailings (not considering the water) at the moment of the accident (IBAMA 2016). The dam structure was composed of an earth fill as start dike with later progressive heightening with sand tailings dikes (Morgenstern et al. 2016). The reservoir stored two kinds of iron ore tailings separately: (1) sand tailings composed of both sand and silt-sized particles and (2) slimes, which are fine grained and clayey (Morgenstern et al. 2016).

Field Measurements

After the Fundão Dam collapse, the hyperconcentrated floodwave went through Santarém Creek, down to the Gualaxo do Norte River and the Carmo River. The floodwave traveled 70 km in the Gualaxo do Norte River plus 25 km in the Carmo River until it reached the Doce River. Through the Doce River, it ran for approximately 570 km until it reached the ocean (ANA 2016b). The flow with high concentration (maximum measured 400,000 mg/L) of suspended material went through four hydropower plant reservoirs, as shown in Fig. 1.

In order to track the impacts of the dam break on the watershed, the Geological Service of Brazil and the National Water Agency conducted several measurements at 10 sites along the Doce River Companhia de Pesquisa de Recursos Minerais and Agência Nacional de Águas (CPRM and ANA 2015; ANA 2017). The first survey occurred immediately after the dam collapse, from November 7 to 23, when the agencies collected data of discharge, water level, temperature, dissolved oxygen, pH, turbidity, particle size, and concentration of sediments in suspension (CPRM and ANA 2015). Fig. 2 shows the relationship obtained between the turbidity in NTU and the sediment concentration in mg/L measured during the event. Turbidity measures the relative water clarity and not the sediment concentration; however, the measurements during the passage of the mud indicated a strong correlation ($R^2 = 0.98$) between sediment concentration and turbidity.

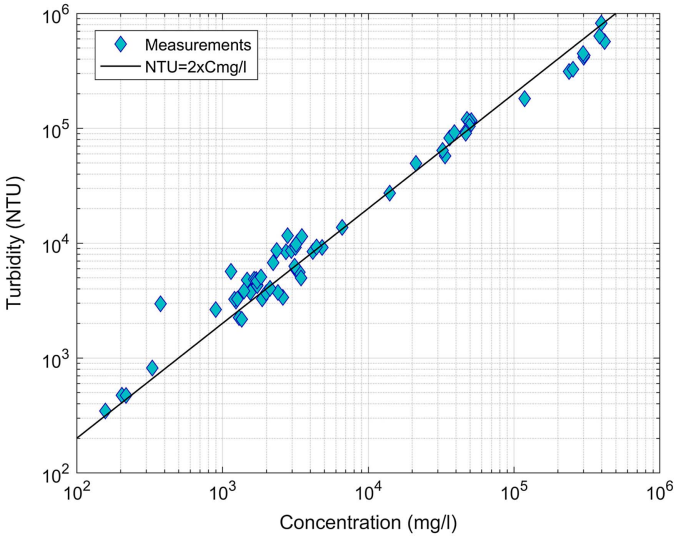

Fig. 2. Observed relationship between turbidity and suspended sediment concentration along the Doce River after the Fundão Dam collapse. (Data from CPRM and ANA 2015.)

According to the survey report, the physical-chemical parameters (temperature, dissolved oxygen, pH, and electrical conductivity) were determined by means of a water quality multiparameter probe (HIDROLAB-MS5, OTT Hydromet, Loveland, Colorado) and the turbidity using a portable turbidimeter (PoliControl-2000, Diadema, Brazil). In addition, the sediment concentration data were collected using instantaneous samplers near the banks, positioned 30 cm deep from the surface. Later, the particle size of the suspended sediment was obtained in the lab (LAMINBH and GEOSOL) by laser scattering using the Laser Granulometer Malvern 2000 (Malvern Panalytical, Westborough, Massachusetts) (CPRM and ANA 2016).

Fig. 1 also presents the river reaches affected by the mud and the location of the data collection sites, including six gauging stations labeled G1 to G6 (where there were measurements of both discharge and sediment concentration) and four additional measurement sites, S1 to S4 (where there were only measurements of sediment concentration). The physical-chemical parameters were collected at all stations. Fig. 3 shows the observed hydrographs and sediment concentration in the main gauging stations along the Doce River.

As one can easily see in Fig. 3, there is lag between the floodwave propagation and suspended sediment transport. This phenomenon happened due to the retarding effect of the hydropower plant reservoirs over the sediment because the floodwave readily passed downstream due to the spillway operation, whereas the sediment passed the reservoir at a slower velocity. Another important observation was the difference between the floodwave celerity and the flow velocity in the fluvial reaches. The floodwave celerity is faster than the flow velocity that carries the sediment (Chanson 2004; Chapra 2008; Julien 2018).

Classification of Sediment Transport

In order to apply an appropriate method to calculate the sediment transport in a river, the first step is to identify the primary mode of sediment transport in terms of bedload or suspended load. The motion of noncohesive bed particles describes bedload transport, which occurs once the shear stress applied on the bed material exceeds the critical shear stress. In general, silt and clay particles enter suspension. Thus, Table 1 presents the modes of sediment

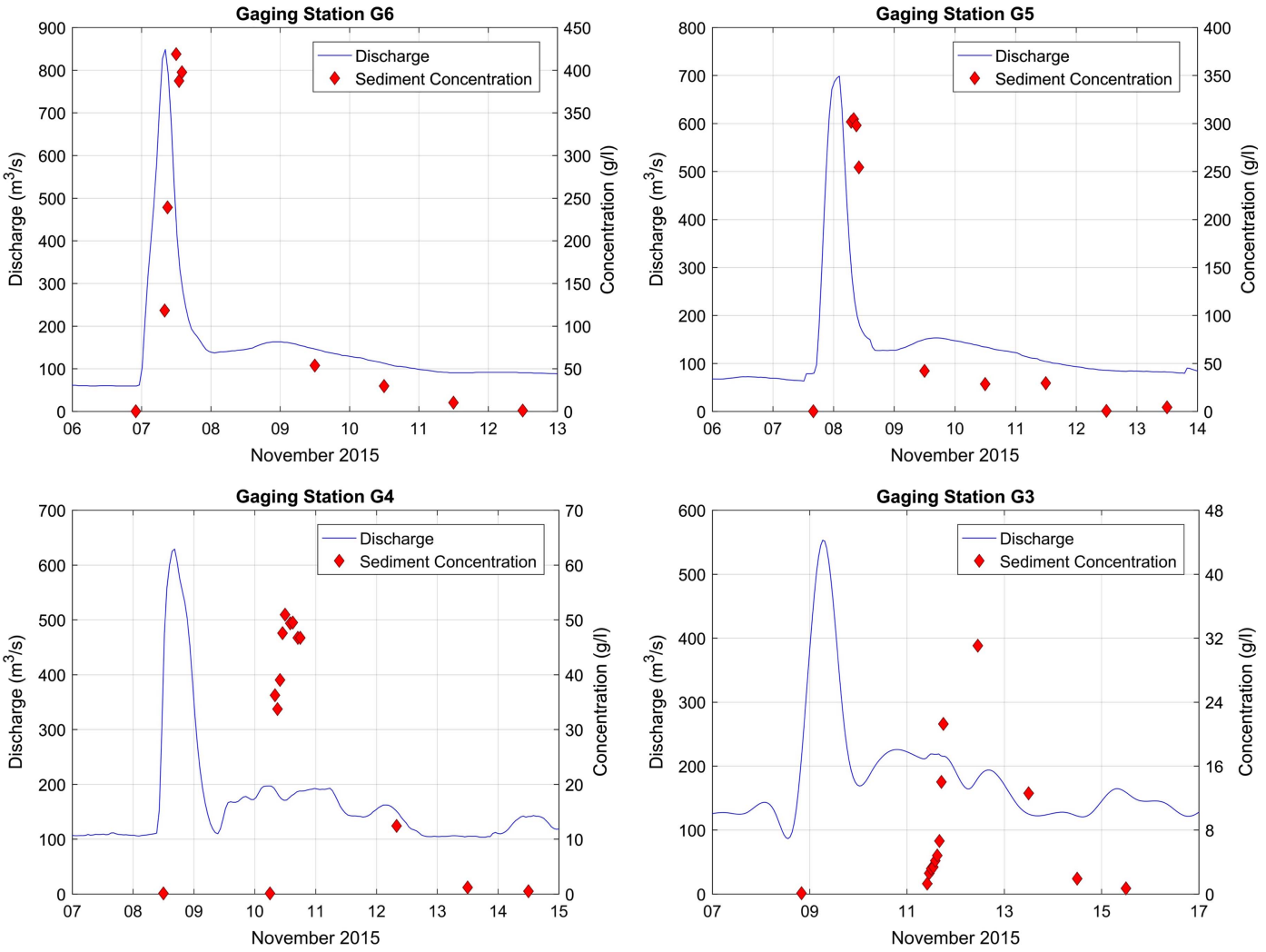

Fig. 3. Observed hydrographs and suspended sediment concentration in the Doce River after the Fundão Dam collapse.

transport as function of the Rouse number, shear, and fall velocities, after Julien (2010). The shear velocity can be calculated as

$$u_* = \sqrt{gR_hS_f} \tag{1}$$

where g = gravitational acceleration. The fall velocity is given by

$$\omega = \frac{8\upsilon_m}{d_s}[(1 + 0.0139d_*^3)^{0.5} - 1] \tag{2}$$

where υ_m = kinematic viscosity of a mixture; d_s = particle diameter; and d_* = dimensionless particle diameter, written as

$$d_* = d_s\left[\frac{(G-1)g}{\upsilon_m^2}\right]^{1/3} \tag{3}$$

where the specific gravity G = ratio between the specific weight of a solid particle and the specific weight of fluid at a standard reference temperature. At a reference temperature of 4°C, the specific gravity of a quartz particle is equal to 2.65. Finally, the Rouse number Ro is equal to

$$Ro = \frac{\omega}{\kappa u_*} \tag{4}$$

where κ = von Karman constant, usually adopted equal to $\kappa = 0.4$.

Table 1. Mode of sediment transport as function of the shear and fall velocities

Ro	u_*/ω	Mode of sediment transport
>12.5	<0.2	No motion
≈12.5	≈0.2	Incipient motion
12.5–5	0.2–0.5	Bedload
5–1.25	0.5–2	Mixed load
1.25–0.5	2–5	Suspension
<0.5	>5	Suspension

Advection-Dispersion Equation

For suspended sediment transport, the general relationship describing conservation of mass for sediment in incompressible dilute suspensions considers advection, diffusion, turbulent mixing, and dispersion, as given by (Julien 2010)

$$\frac{\partial C}{\partial t} + v_x\frac{\partial C}{\partial x} + v_y\frac{\partial C}{\partial y} + v_z\frac{\partial C}{\partial z} = \dot{C} + (d+\varepsilon_x)\frac{\partial^2 C}{\partial x^2} + (d+\varepsilon_y)\frac{\partial^2 C}{\partial y^2} + (d+\varepsilon_z)\frac{\partial^2 C}{\partial z^2} \tag{5}$$

where C = volume-average sediment concentration inside the infinitesimal control volume; v_x, v_y, v_z = flow velocities in the x, y, and z directions, respectively; $\dot{C}$ = rate of sediment reaction per unit volume; d = molecular diffusion coefficient (usually negligible); and ε = turbulent mixing coefficient, describing the process of turbulent diffusion.

For a one-dimensional turbulent flow, the coefficient d will vanish, as well as the terms ε_y and ε_z in the y and z directions. A practical application of the previously mentioned equation is the case of the accidental spill of a pollutant into a river. Thus, the propagation of a contaminant or suspended load can be properly modeled by the one-dimensional advection-dispersion equation (Fischer et al. 1979; Rutherford 1994; Chanson 2004; Chapra 2008; Julien 2018)

$$\frac{\partial C}{\partial t} + U\frac{\partial C}{\partial x} = K_d\frac{\partial^2 C}{\partial x^2} - kC \tag{6}$$

where U = cross sectional averaged velocity; K_d = longitudinal dispersion coefficient; and k = settling rate or rate of sediment deposition. Longitudinal dispersion occurs only after the vertical and lateral mixing are complete; thus, the application of Eq. (6) is valid only when the concentration is uniform within a cross-section. For the particular case of mine tailings collapse, dispersion starts immediately because the vertical and lateral mixing are both complete at the source.

In order to solve Eq. (6), several researchers have developed empirical expressions to estimate the longitudinal dispersion coefficient as function of hydraulic and geometric river parameters (Fischer et al. 1979; Rutherford 1994; Seo and Cheong 1998; Kashefipour and Falconer 2002; Tayfur and Singh 2005; Zeng and Huai 2014). Despite the availably of several formulations to obtain the longitudinal dispersion coefficient, the literature presents only few practical applications of such developed equations.

Table 2 presents some of the most recent developments of empirical equations for the prediction of longitudinal dispersion coefficient (Julien 2010; Kashefipour and Falconer 2002; Zeng and Huai 2014), where h = flow depth and W = river width. Moreover, another required parameter of Eq. (6) is the settling rate k, which is given by

$$k = \frac{\omega_i}{h} \tag{7}$$

where ω_i = fall velocity for the sediment fraction i.

Table 2. Empirical equations for the prediction of longitudinal dispersion coefficient

ID	Expression	Author
1	$K_d = 10.612(U/u_*)hU$	Kashefipour and Falconer (2002)
2	$K_d = 250hu_*$	Julien (2010)
3	$K_d = 5.4(W/h)^{0.7}(U/u_*)^{0.13}hU$	Zeng and Huai (2014)

Suspended Sediment Retention in a Reservoir

Taking into account the conservation of mass applied to sediment and assuming a steady supply of sediment in one-dimensional flow, Julien (2010) shows that the relationship between the concentration upstream and downstream of a reservoir can be written as

$$C_i = C_{oi}e^{\frac{-X\omega_i}{hU}} \tag{8}$$

where C_i and C_{oi} = sediment concentration downstream and upstream, respectively. This expression is in good agreement with the measurements carried out by Cecen (1969). In addition, the trap efficiency, or, in other words, the percentage of sediment fraction i that settles within a distance X, is equal to

$$T_{Ei} = \frac{C_{oi} - C_i}{C_{oi}} = 1 - e^{\frac{-X\omega_i}{hU}} \tag{9}$$

Also, substituting Eq. (7) into Eq. (9) and considering the time $t = X/U$

$$T_{Ei} = 1 - e^{-kt} \tag{10}$$

As expected, the settling conditions in rivers and reservoirs are compatible.

Analytical Solution for the One-Dimensional Advection-Dispersion Equation

For the specific case where the spill concentration is kept constant for a finite time interval, as illustrated in Fig. 4(a), the analytical solution of Eq. (6) is given by the following expression (Chapra 2008):

$$C(x,t) = \frac{C_0}{2}\left\{e^{\frac{Ux}{2K_d}(1-\Gamma)}\left[\operatorname{erfc}\left(\frac{x - Ut\Gamma}{2\sqrt{K_d t}}\right) - \operatorname{erfc}\left(\frac{x - U(t-T_s)\Gamma}{2\sqrt{K_d(t-T_s)}}\right)\right]\right.$$
$$\left. + e^{\frac{Ux}{2K_d}(1+\Gamma)}\left[\operatorname{erfc}\left(\frac{x + Ut\Gamma}{2\sqrt{K_d t}}\right) - \operatorname{erfc}\left(\frac{x + U(t-T_s)\Gamma}{2\sqrt{K_d(t-T_s)}}\right)\right]\right\} \tag{11}$$

where C_0 = initial concentration; t = elapsed time after the spill; and T_s = spilling duration time. This equation also includes two additional parameters

$$\Gamma = \sqrt{1 + 4\eta} \tag{12}$$

and

$$\eta = \frac{kK_d}{U^2} \tag{13}$$

The complementary error function, erfc, is equal to 1 minus the error function, where the error function is the following integral:

$$\operatorname{erf}(b) = \frac{2}{\sqrt{\pi}}\int_0^b e^{-\beta^2}d\beta \tag{14}$$

where β = dummy variable.

The error function is available from different sources, such as standard software libraries [International Math and Statistics Library (IMSL)] and Numerical Recipes (Press et al. 2007), and can be directly calculated from several software packages, including Microsoft Excel. Nevertheless, this analytical solution has a numerical restriction due to the second term in the right hand side of the equation because the exponential can tend to infinity,

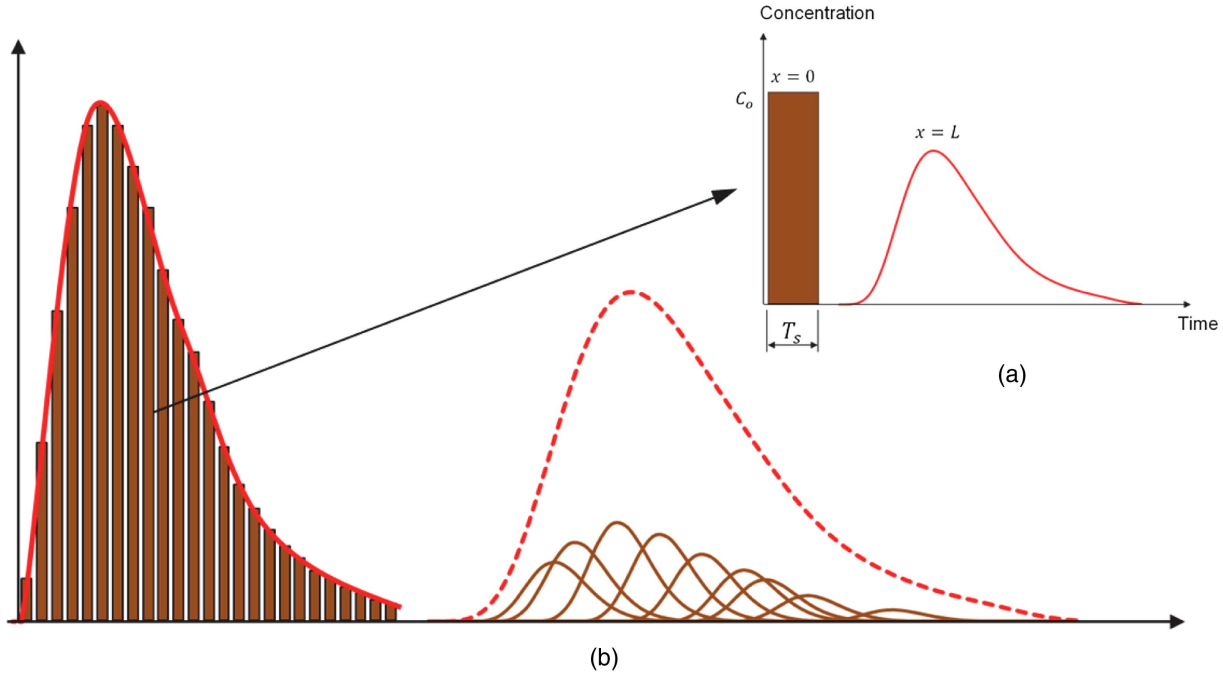

Fig. 4. Analytical solution and application of the superposition principle.

blowing up the solution for long river reaches. Thus, the maximum practical reach length L in which Eq. (11) is applicable is restricted to

$$L \leq 700 \frac{K_d}{U} \tag{15}$$

Modeling of Suspended Sediment Transport

Identification of the Dominant Mode of Sediment Transport

The definition of the primary mode of sediment transport along the Doce River after the dam break could be carried out considering the measured discharge, sediment particle size, and river cross-section geometry. Table 3 presents the measurements and the parameters calculated using Eqs. (1)–(4). The analysis result points out that the prime mode of sediment transport is suspension for the whole extension of the Doce River; therefore, the advection-dispersion equation should be a proper approach to evaluate the suspended sediment propagation.

Calibration of the Advection-Dispersion Equation Parameters

The practical application of the advection-dispersion equation is associated with cases of the transport of pollutants or sediment in suspension. According to Fischer et al. (1979), observed values for the longitudinal dispersion coefficient in real streams can be obtained through the routing procedure. This procedure consists of solving Eq. (6) in order to match a downstream observation of a passage of a tracer cloud based on an upstream observation. The value of K_d is varied to obtain the best fit between the observed and predicted downstream curves, with the best fit value regarded as the observed longitudinal dispersion coefficient (Fischer et al. 1979). However, herein, the procedure for conservative substances has been modified to incorporate the case of sediment settling by the application of the analytical solution to Eqs. (11)–(13).

First, the analytical solution of advection-dispersion equation requires the discretization of the concentration time-varying series in short duration blocks, representing the spilling duration time T_s in Eq. (11). After that, the application of the superposition principle takes place, as illustrated in Fig. 4(b). There is no numerical diffusion involved when the analytical solution is applied (rather than numerical solutions) to solve the advection-dispersion equation.

The adapted routing method was applied to the Doce River after the Fundão Dam collapse in reaches where there were measured sediment concentrations. No significant improvement on the calculations was observed for the blocks (spilling duration time) with duration shorter than 1 h; therefore, that was the discretization adopted. Furthermore, the methodology considers that the longitudinal dispersion coefficient and the settling rate are constant along each reach.

Table 3. Classification of sediment transport mode in the Doce River after the Fundão Dam failure

Location	Q (m^3/s)	W (m)	S_o	h (m)	u_* (m)	d_{50} (μm)	d_*	ω (mm/s)	u_*/ω	Ro	Mode of sediment transport
G6	150	150	0.0005	0.89	0.07	18.1	0.53	0.37	180	0.014	Suspension
G5	130	240	0.0005	0.48	0.05	17.9	0.50	0.34	145	0.017	Suspension
G4	141	320	0.0005	1.26	0.08	6.6	0.19	0.05	1601	0.002	Suspension
G3	182	400	0.0005	1.23	0.08	7.7	0.23	0.07	1165	0.002	Suspension
G2	309	630	0.0002	1.37	0.05	5.9	0.17	0.04	1358	0.002	Suspension
G1	350	810	0.0002	0.86	0.04	6.0	0.17	0.04	1043	0.002	Suspension

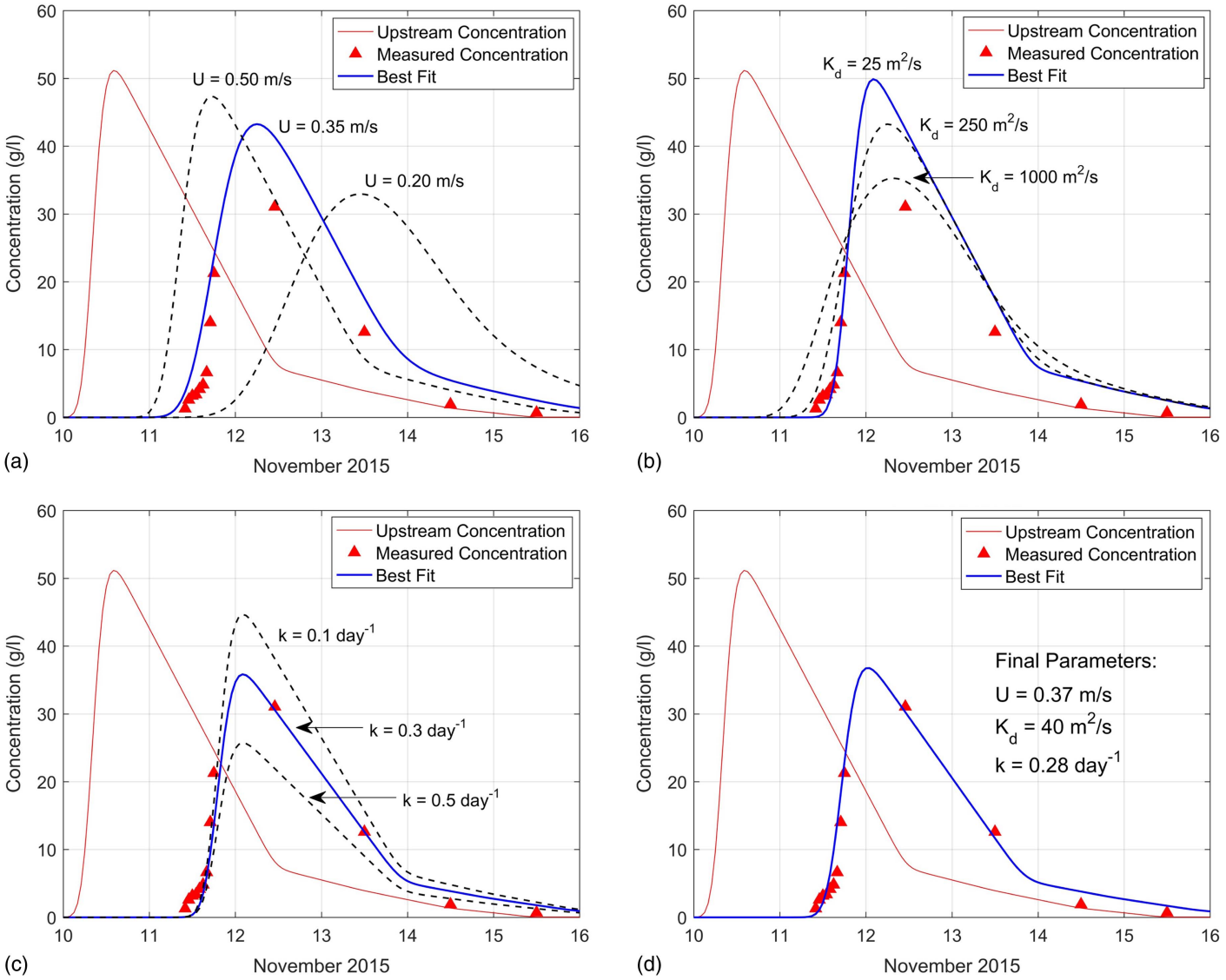

Fig. 5. Example of procedure applied on the Doce River between stations G4 and G3 to determine the advection-dispersion parameters using the one-dimensional analytical equation: (a) advection parameter; (b) dispersion parameter; (c) setting parameter; and (d) refinement.

Table 4. Calculation of the advection-dispersion equation parameters in the Doce River

Hydraulic and geometric parameters						Calibrated parameters			
Reach	Distance (km)	S_o	W (m)	h (m)	u_* (m/s)	U (m/s)	K_d (m^2/s)	k (day^{-1})	R^2
G6–G5	73.6	0.00050	195	0.69	0.06	1.12	120	0.33	0.91
G5–Reservoir	34.9	0.00050	260	0.45	0.05	1.12	120	0.33	—
Reservoir–G4	25.3	0.00050	303	1.33	0.08	0.35	35	0.29	0.96
G4–G3	43.4	0.00050	360	1.37	0.08	0.37	40	0.28	0.92
G3–S4	64.0	0.00050	434	1.15	0.08	0.37	40	0.28	0.85
Reservoir–S3	11.5	0.00080	536	1.08	0.09	0.35	30	0.11	0.82
Reservoir–S2	6.7	0.00080	622	1.07	0.09	0.35	30	0.11	0.78
S2–G2	27.5	0.00080	627	1.38	0.10	0.36	30	0.11	0.76
G2–G1	64.7	0.00020	720	0.97	0.04	0.50	50	0.21	0.88
G1–S1	39.0	0.00020	815	0.86	0.04	0.50	50	0.21	0.96

At gauging station G6, the concentration was linearly interpolated from the observed values. For the subsequent reaches, the calculated concentration in the downstream gauging station served as input for the next reach. The adjustment of the advection, dispersion, and settling parameters targeted the best fit with the measured data during the event, using the highest determination coefficient R^2 as the objective function.

Fig. 5 illustrates the process to determine the equation parameters, taking the river reach between gauging stations G4–G3 as exemplification. At the beginning, the flow velocity (advection

J. Hydraul. Eng., 2019, 145(5): 05019002

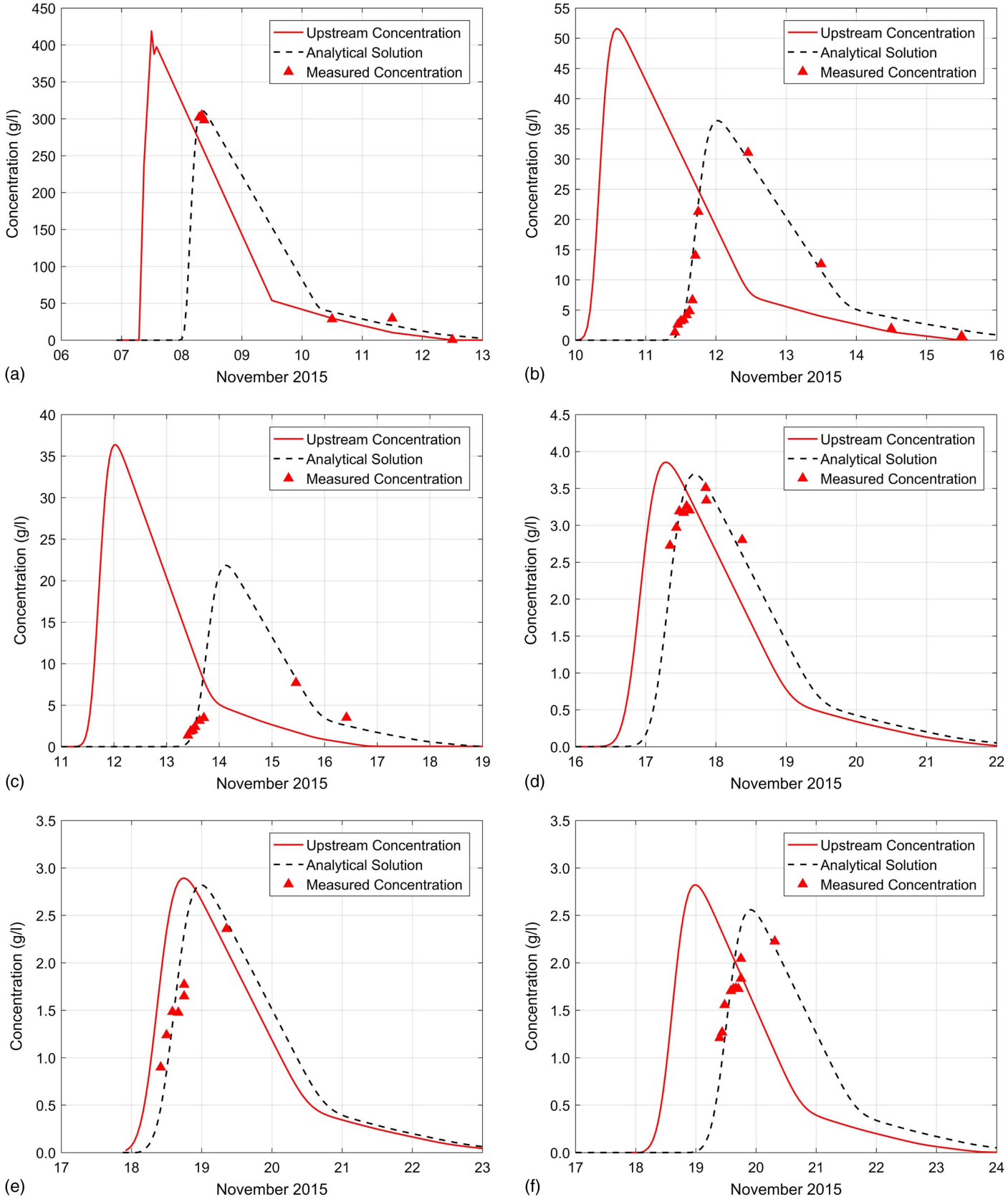

Fig. 6. Comparison between the observed concentrations in the Doce River and the one-dimensional analytical equation after the calibration of the advection-dispersion equation parameters: (a) routing procedure: reach G6–G5; (b) reach G4–G3; (c) reach G3–S4; (d) Aimorés reservoir-S3; (e) Mascarenhas reservoir-S2; and (f) reach S2–G2.

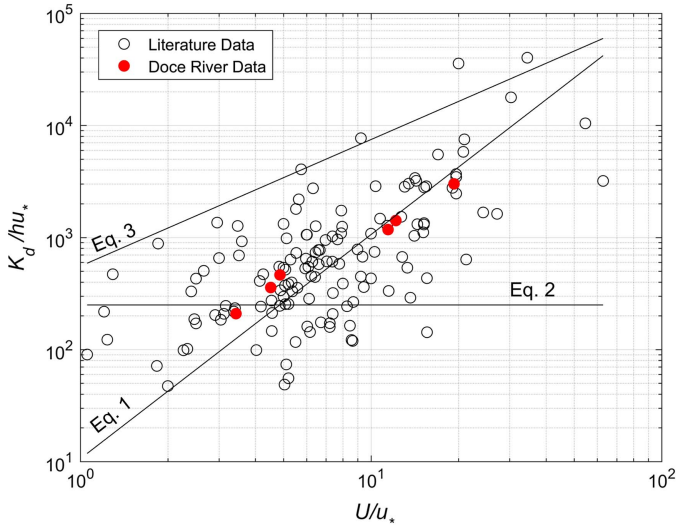

Fig. 7. Comparison among the literature, Doce River data, and empirical expression to predict the longitudinal dispersion coefficient.

parameter) is varied to approximate the analytical solution to the measured concentration [Fig. 5(a)]. For this step, an initial guess for the longitudinal dispersion coefficient K_d is taken (here $K_d = 250$ m^2/s), and the settling rate k is assumed to be equal to zero (conservative substance).

Afterward, the flow velocity corresponding to the best fit is retained for the next step, which is the determination of K_d (dispersion parameter). Similarly, K_d varies in order to approximate the calculation of the observed values, as showed in Fig. 5(b). After these two initial steps, one can see that the flow velocity and K_d parameters are not sufficient to fit the measured data. Clearly, this occurs due the sediment deposition between stations G4 and G3. Thus, the next parameter to be adjusted is the settling rate k [Fig. 5(c)], conserving the parameters obtained in the two previous steps. To conclude the procedure, a refinement takes place in order to achieve the highest determination coefficient R^2.

Finally, Table 4 summarizes the parameters calibrated in the Doce River, whereas Fig. 6 shows the comparison of the analytical equation with the measured data in the stations. For the reaches where there are reservoirs between the observed concentrations, Eq. (8) was applied, using the reservoir data from the Brazilian National Water Agency (ANA 2016a) and the National Electrical System Operator (ONS 2017). In this case, a similar procedure presented in Fig. 5 is employed; however, now the variables to be adjusted are the settling rate and the time for the sediment to cross the reservoir.

Despite the Doce River width (varying from 200 to 800 m), the analytical equation presented satisfactory agreement with the observed concentrations at all stations, indicating that the analytical equations can be employed as one-dimensional modeling for the suspended sediment propagation on similar cases, both for the river reaches and reservoirs. The good results using the one-dimensional model can be attributed to the massive amount of sediment dumped in the river and due to the effect of the spillways along the river, which acted as mixers, promoting vertical and lateral mixing in the river reaches.

Longitudinal Dispersion Coefficient Evaluation

Now, in order to check the relevance of the calibration parameters found in the Doce River after the dam collapse, Fig. 7 shows data of 141 points from 50 rivers in the United States and New Zealand found in the literature (McQuivey and Keefer 1974; Fischer et al. 1979; Seo and Cheong 1998; Deng et al. 2001; Kashefipour and Falconer 2002; Carr and Rehmann 2007; Zeng and Huai 2014) using the dimensionless parameters K_d/hu_* and U/u_* for comparison. In addition, the expressions developed by Kashefipour and Falconer (2002), Julien (2010), and Zeng and Huai (2014) are plotted in the same graph considering the average ratio width-depth found in the Doce River $W/h \approx 500$. The corresponding equations are also found in Table 2.

One can realize that there is good agreement between the literature and the Doce River data because the observed points follow the same trend, despite the variability in dispersion coefficients reported in the literature.

Furthermore, among the empirical expressions tested for the longitudinal dispersion coefficient estimation, the formulation developed by Kashefipour and Falconer (2002) presented the best fit with the literature and Doce River data. Therefore, this formulation was retained for further modeling applications, where K_d can be predicted reasonably using hydraulic and geometric parameters.

Sediment Settling Rate Evaluation

The other parameter required in the solution of the advection-dispersion equation is the sediment settling rate k. This is a relatively new parameter that depends on the fall velocity of a specific particle size. After the calibration of the settling rates based on the measurements carried out in the Doce River (Table 4), the identification of the representative diameter of the settling rate observed in the Doce River could be obtained by the application of Eq. (7). This calculation takes into account the measured flow depth and water temperature. Table 5 provides the calculated

Table 5. Determination of the particle sizes associated with the observed settling rate along the Doce River

Reach	Settling rate, k (day^{-1})	Water temperature (°C)	Fall velocity, ω (mm/s)	Dimensionless diameter, d_*	Calculated particle size, d_s (μm)
G6–G5	0.33	30.00	0.0026	0.04	1.52
G5–Reservoir	0.33	27.00	0.0017	0.04	1.27
Reservoir–G4	0.29	30.00	0.0045	0.06	2.00
G4–G3	0.28	30.00	0.0044	0.06	1.97
G3–S4	0.28	31.00	0.0037	0.05	1.84
Reservoir–S3	0.11	29.00	0.0014	0.03	1.13
Reservoir–S2	0.11	29.00	0.0014	0.03	1.13
S2–G2	0.11	29.00	0.0018	0.04	1.28
G2–G1	0.21	29.00	0.0023	0.04	1.46
G1–S1	0.21	29.00	0.0021	0.04	1.37

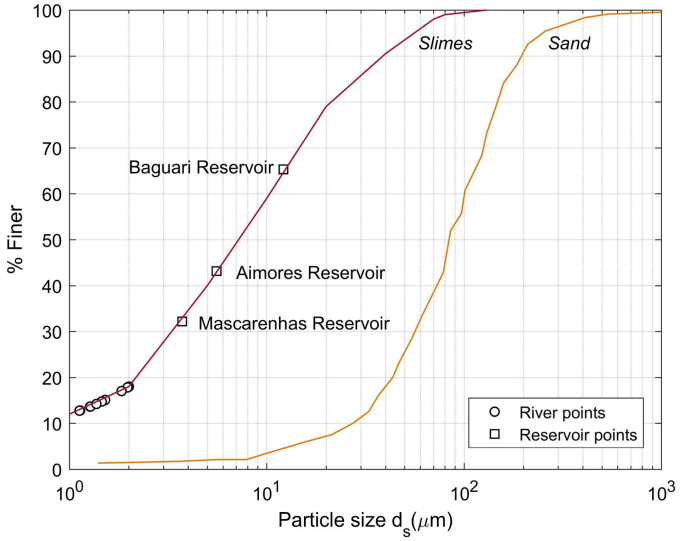

Fig. 8. Comparison between the particle size distribution of the material stored in the Fundão Dam reservoir and the particle size associated with the settling rate observed in the Doce River reaches and reservoirs.

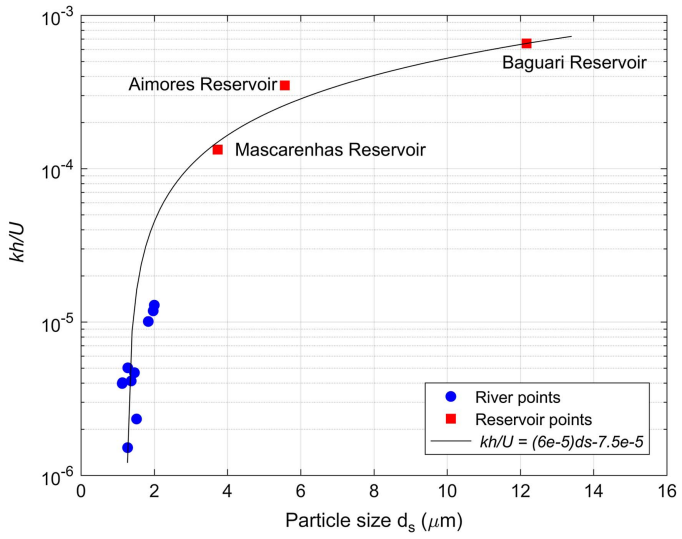

Fig. 9. Dimensionless settling parameter as function of the representative particle size.

diameter associated with the settling rate observed along the Doce River.

According to the analysis, the particle size corresponding to the settling rate ranged from 1.1 to 2.0 μm, which classifies the sediment as medium to coarse clay. This result is remarkably consistent along the whole extension of Doce River (570 km) and denotes that the sediment settling rates are clearly related to the slimes (finer tailings) of the Fundão Dam, which remained in suspension and sustained high turbidity levels in the river. These representative diameters are smaller than the d_{50} observed in the stations (Table 3) because the sediment concentration decays only after the settling of the fine particles in suspension, which are smaller than d_{50}.

Fig. 8 illustrates the particle diameter corresponding to the settling rate in the Doce River compared to the particle size distribution of the material stored at Fundão Dam. From this comparison, one can conclude that the diameter related to the sediment settling rate observed in the Doce River corresponds approximately to d_{15} of the slimes of the Fundão Dam.

In reservoirs, the application of Eq. (8) considering the observed sediment concentration data upstream and downstream of each reservoir provided the representative particle size of the settling rate in the reservoirs. For this calculation, the temperature in the reservoir was assumed to be equal to the average water temperature measured on river reaches upstream and downstream of the reservoir. Table 6 presents a summary of the parameters for the sediment routing in the reservoir and the observed d_{50} in the upstream gauging stations. Accordingly, the representative settling rate observed in each reservoir is related to particle diameters slightly finer relative to the d_{50} of the observed particles upstream of the reservoirs because, differently from the river reaches, it traps the coarse material more efficiently. Thus, the particle size decreased as the flood wave passed through successive reservoirs from Baguari and Aimorés to Mascarenhas Reservoirs (Fig. 1).

Because the same settling rate is applicable in the river and the reservoirs, it is possible to define the settling rate as a function of the dimensionless parameter kh/U. Fig. 9 illustrates the relationship between the particle size and the dimensionless parameter obtained for the Doce River reaches and reservoirs.

Simulation of the Suspended Sediment Transport along the Doce River after the Fundão Dam Collapse

The calibration of the advection-dispersion parameters enabled the simulation of the sediment concentration over the entire Doce River from gauging station G6 to the ocean, as presented in Fig. 10. In order to provide a practical visualization of the impact caused by the collapse, this figure also shows the estimated maximum acceptable turbidity level at the water treatment plant intakes (WTP) along the Doce River. According to Chang and Liao (2012), turbidity levels higher than 5,000 NTU hinder water treatment; thus, based on the measurements presented in Fig. 2, this turbidity corresponds to a sediment concentration of ~2,500 mg/L in the Doce River. From this illustration, one can easily see the consequences in the water supply in the downstream populations. As registered by the Brazilian agencies (ANA 2016b), the high turbidity resulted in the interruption of water supply for several days, affecting 424,000 people. As an example, according to the local media in Governador Valadares City (the same location as gauging station G4), with approximately 270,000 inhabitants, the

Table 6. Determination of the particle size associated with the observed settling rate in the Doce River reservoirs

Reservoir	Extension (km)	U (m/s)	Depth (m)	k (day^{-1})	ω (mm/s)	Representative particle size determined, d_s (μm)	Particle size d_{50} observed upstream (μm)
Baguari	22.0	0.25	10.0	1.40	0.1605	12.2	17.9
Aimorés	27.3	0.10	5.5	0.55	0.0349	5.6	7.4
Mascarenhas	10.4	0.12	5.0	0.23	0.0133	3.5	4.0

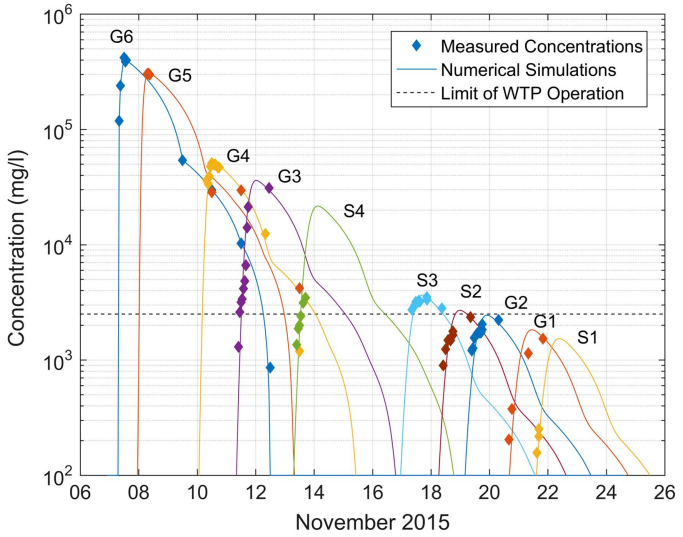

Fig. 10. Simulation of the sediment concentration along the Doce River after the Fundão Dam collapse.

water supply was interrupted for 8 days, from November 8 to November 16, 2015.

Now, the following topics present a sensitivity analysis regarding the effects of reservoirs and water temperature on sediment propagation and settling.

Effect of Hydropower Plant Reservoirs on Sediment Propagation

The observed suspended sediment concentration in the gauging stations along the Doce River emphasized the essential role of hydropower plant reservoirs in trapping the sediment and reducing the concentration further downstream.

According to the Brazilian Institute of Environment and Renewable Natural Resources, the Candonga reservoir trapped 7 million cubic meters of tailings immediately after the accident (IBAMA 2016). This represents approximately 20% of the total sediment released from Fundão Dam.

In the Doce River, the estimated sediment yield could be obtained from the observed concentrations and discharges in the gauging stations. Fig. 11 presents an estimated volume of sediment at Doce River stations and the trap efficiency for each Doce River reach and for the reservoirs, based on Eqs. (9) and (10). According to the measurements, the volumes trapped in the Doce River reservoirs were approximately: Baguari 2 Mm^3, Aimorés 0.1 Mm^3, and Mascarenhas 0.01 Mm^3.

Model simulations can now determine what the concentration in the Doce River would have been without the interference of the Baguari, Aimorés, and Mascarenhas reservoirs in the Doce River. The simulation starts at gauging station G6, using the measured sediment data as the upstream boundary condition. The Doce River was divided into nine reaches, approximately simulating the conditions of the river during the passage of the sediment; the extension of each reach is limited by Eq. (15). The equation developed by Kashefipour and Falconer (2002) was applied to predict the longitudinal coefficient using hydraulic parameters (flow velocity, depth, and shear velocity). The settling rate is calculated using the using Eqs. (2), (3), and (7), assuming a constant particle size equal to 1.5 μm. This diameter corresponds to the average diameter associated with the observed settling rate along the Doce River.

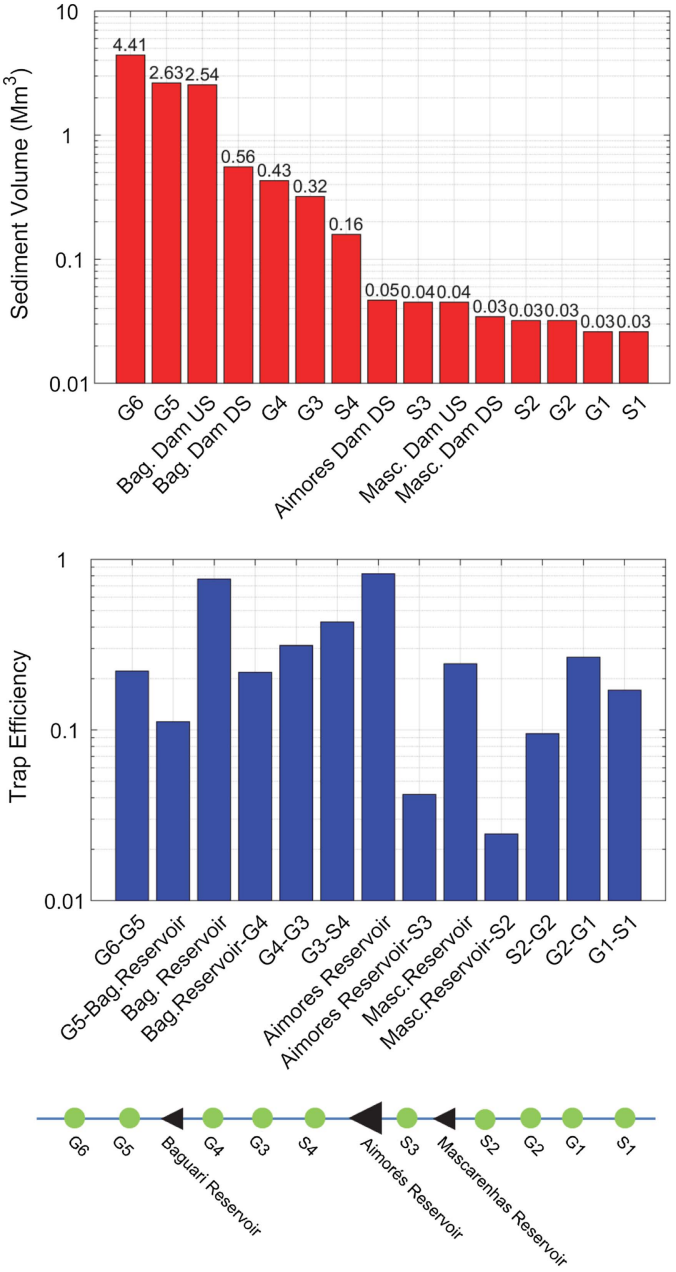

Fig. 11. Estimative of passing sediment volume and the trap efficiency along the Doce River and reservoirs.

Table 7 summarizes the parameters used in the Doce River simulation for the hypothetical situation of the sediment propagation without the Baguari, Aimorés, and Mascarenhas hydropower reservoirs. In addition, Fig. 12 presents the hypothetical sediment concentrations along the Doce River without the previously mentioned reservoirs.

As one can conclude, the reservoirs dramatically decreased the sediment concentration along the river. Without these dams, the sediment concentration at the coast would have reached a maximum peak of approximately 64,000 mg/L, rather than the observed 1,500 mg/L. In addition, the higher concentrations would have caused more environmental damage at the location of the downstream gauging stations (S3 to S1) and caused a more extensive disturbance in water supply operations due to high turbidity along the lower river reaches.

Table 7. Simulation of the sediment propagation along the Doce River without the interference of three hydropower reservoirs (Baguari, Aimorés, and Mascarenhas)

Reach	Length (km)	Accumulated (km)	S_o	U (m/s)	h (m)	u_* (m/s)	K_d (m^2/s)	d_s (μm)	d_*	Temperature (°C)	ν_m (m^2/s)	ω (mm/s)	k (day^{-1})
R1	50	50	0.00050	1.00	1.00	0.07	152	1.50	0.04	29.00	8.20E–07	0.0025	0.21
R2	50	100	0.00050	1.00	1.00	0.07	152	1.50	0.04	29.00	8.20E–07	0.0025	0.21
R3	50	150	0.00050	0.40	1.50	0.09	30	1.50	0.04	29.00	8.20E–07	0.0025	0.14
R4	50	200	0.00050	0.40	1.50	0.09	30	1.50	0.04	29.00	8.20E–07	0.0025	0.14
R5	50	250	0.00050	0.40	1.50	0.09	30	1.50	0.04	29.00	8.20E–07	0.0025	0.14
R6	40	290	0.00080	0.40	1.50	0.11	23	1.50	0.04	29.00	8.20E–07	0.0025	0.14
R7	55	345	0.00020	0.40	1.00	0.04	38	1.50	0.04	29.00	8.20E–07	0.0025	0.21
R8	55	400	0.00020	0.50	1.00	0.04	60	1.50	0.04	29.00	8.20E–07	0.0025	0.21
R9	55	455	0.00020	0.50	1.00	0.04	60	1.50	0.04	29.00	8.20E–07	0.0025	0.21

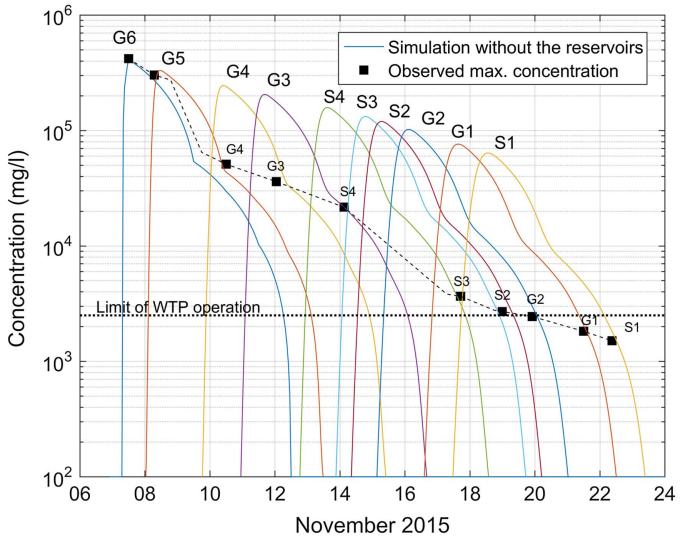

Fig. 12. Suspended sediment simulation in Doce River considering the hypothesis of the inexistence of three hydropower reservoirs. (Baguari, Aimorés, and Mascarenhas.)

Effect of Temperature on Suspended Sediment Propagation

As presented earlier, the particle size related to the settling rate can be classified as medium to coarse clay, which suggests the dependency of the settling rate on the water temperature (Julien 2010).

In order to evaluate the potential impact of water temperature changes, Table 8 presents the settling rate along the Doce River for the average measured water temperature ($T \cong 29$°C) as well as colder temperatures ($T = 20$°C, $T = 10$°C, and $T = 5$°C). This table considers that all other parameters on the river (flow velocity, flow depth, longitudinal dispersion coefficient, and particle size) remained exactly the same as measured. The results of this evaluation for each station are shown in Fig. 13.

As expected, this sensitivity analysis shows that the decrease in the water temperature directly affects the settling rate. Thus, the warm water temperature accelerates the sediment deposition along the river, whereas cold water retards it. For a hypothetical temperature of $T = 5$°C, the concentration on the Brazilian coast would have been approximately 12 times higher than the observed one.

One can conclude that rivers subjected to spilling in cold regions are more susceptible to slow deposition, demanding more time and extension to reduce the concentration of the suspended sediments. On the other hand, warm waters in tropical regions, such as the Doce River, result in faster deposition.

Table 8. Sensitivity analysis of the effect of the temperature over the settling rate

	k (day^{-1})			
Reach	$T = 29$°C measured temperature	$T = 20$°C	$T = 10$°C	$T = 5$°C
G6–G5	0.33	0.26	0.20	0.17
G5–Reservoir	0.33	0.28	0.22	0.19
Reservoir–G4	0.29	0.24	0.18	0.16
G4–G3	0.28	0.22	0.17	0.15
G3–S4	0.28	0.23	0.17	0.15
Reservoir–S3	0.11	0.09	0.07	0.06
Reservoir–S2	0.11	0.09	0.07	0.06
S2–G2	0.11	0.09	0.07	0.06
G2–G1	0.21	0.17	0.13	0.11
G1–S1	0.21	0.17	0.13	0.11
Reservoir				
Res. Baguari	1.40	1.16	0.89	0.77
Res. Aimorés	0.55	0.44	0.34	0.29
Res. Mascarenhas	0.27	0.22	0.17	0.15

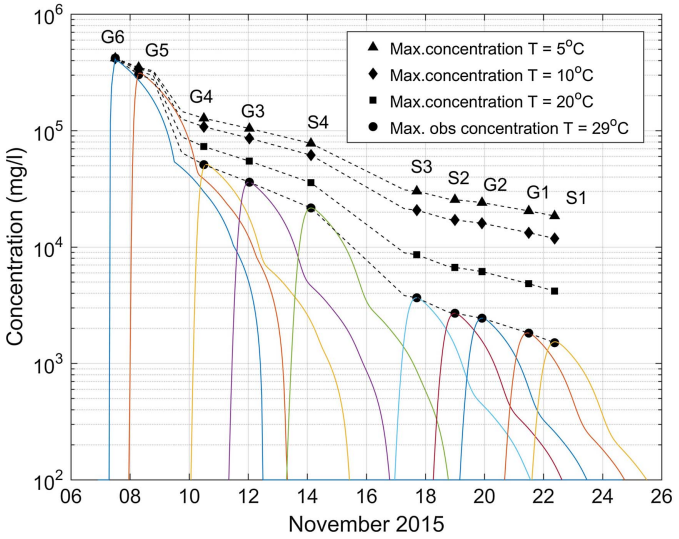

Fig. 13. Suspended sediment simulation considering the effect of temperature on sediment concentration in Doce River.

Conclusion

The sediment wave propagation in the Doce River after the Fundão Dam collapse was modeled using the one-dimensional

advection-dispersion equation, based on the observed concentrations along the river after the accident. Initially, the analytical solution was employed to obtain two main equation parameters: the longitudinal dispersion coefficient and the settling rate. The values found for the longitudinal dispersion coefficient varied from 30 to 120 m^2/s, fitting the literature data, whereas the settling rate relates to particle size ranging from 1.1 to 2.0 μm, clearly associated with the fine material stored at Fundão Dam.

Furthermore, the analytical solution of the advection-dispersion equation was employed to simulate sediment propagation without three hydropower reservoirs (Baguari, Aimorés, and Mascarenhas). Accordingly, the concentration at the coast would have been extensively higher, that is, approximately 64,000 mg/L, instead of the 1,500 mg/L observed, which emphasizes the significance of the reservoirs in sediment trapping.

Finally, a sensitivity analysis with a hypothetical decrease in the water temperature at 25°C would have caused a concentration 12 times higher at the coast. This is due to the large effect of water temperature on fine sediment settling.

Acknowledgments

The authors would like to acknowledge that this work is being developed with the support of CNPq (Brazilian National Council for Scientific and Technological Development).

References

ANA (Agência Nacional de Águas). 2016a. "SAR—Sistema de Acompanhamento de Reservatórios." Accessed April 12, 2016. http://sar.ana.gov.br/.

ANA (Agência Nacional de Águas). 2016b. "Encarte especial sobre a bacia do Rio Doce—Rompimento da barragem em Mariana/MG." In *Conjuntura dos Recursos Hidricos no Brasil—Informe 2015*, 50. Brasília, Brazil: Superintendência de Planejamento de Recursos Hídricos.

ANA (Agência Nacional de Águas). 2017. "HidroWeb." Accessed June 23, 2017. http://hidroweb.ana.gov.br/default.asp.

Armanini, A., L. Fraccarollo, and G. Rosatti. 2009. "Two-dimensional simulation of debris flows in erodible channels." *Comput. Geosci.* 35 (5): 993–1006. https://doi.org/10.1016/j.cageo.2007.11.008.

Azam, S., and Q. Li. 2010. "Tailings dam failures: A review of the last one hundred years." *Geotech. News Mag.* 28 (4): 50–53.

Caldwell, J. A., F. Oboni, and C. Oboni. 2015. "Tailings facility failures in 2014 and an update on failure statistics." In *Proc., Tailings and Mine Waste 2015*. Vancouver, Canada: Univ. of British Columbia.

Carr, M. L., and C. R. Rehmann. 2007. "Measuring the dispersion coefficient with acoustic Doppler current profilers." *J. Hydraul. Eng.* 133 (8): 977–982. https://doi.org/10.1061/(ASCE)0733-9429(2007)133:8(977).

Cecen, K. M. 1969. "Distribution of suspended matter and similarity criteria in settling basins." In *Proc., 13th Congress IAHR*, 215–225. Baden, Germany: International Association for Hydro-Environment Engineering and Research.

Chang, C.-L., and C.-S. Liao. 2012. "Assessing the risk posed by high-turbidity water to water supplies." *Environ. Monit. Assess.* 184 (5): 3127–3132. https://doi.org/10.1007/s10661-011-2176-6.

Chanson, H. 2004. *Environmental hydraulics for open channel flows*. Amsterdam, Netherlands: Butterworth-Heinemann.

Chapra, S. C. 2008. *Surface water-quality modeling*. Long Grove, IL: McGraw-Hill.

CPRM and ANA (Companhia de Pesquisa de Recursos Minerais and Agência Nacional de Águas). 2015. *Monitoramento Especial da Bacia do Rio Doce. Primeira Campanha de Campo, Acompanhamento da onda de cheia*, 33. Belo Horizonte, Brazil: Serviço Geológico do Brasil—Agência Nacional de Águas.

CPRM and ANA (Companhia de Pesquisa de Recursos Minerais and Agência Nacional de Águas). 2016. *Monitoramento Especial da Bacia do Rio Doce. Terceira Campanha de Campo, Monitoramento Simultâneo ao longo de 15 dias*, 84. Belo Horizonte, Brazil: Serviço Geológico do Brasil—Agência Nacional de Águas,.

Davies, M. 2002. "Tailings impoundment failures: Are geotechnical engineers listening?" *Geotech. News* 20 (3): 31–36.

Davies, M., T. Marting, and L. Peter. 2000. *Mine tailings dams: When things go wrong*, 261–273. Las Vegas: Association of State Dam Safety Officials, US Committee on Large Dams.

Deng, Z.-Q., V. P. Singh, and L. Bengtsson. 2001. "Longitudinal dispersion coefficient in straight rivers." *J. Hydraul. Eng.* 127 (11): 919–927. https://doi.org/10.1061/(ASCE)0733-9429(2001)127:11(919).

do Carmo, F. F., et al. 2017. "Fundão tailings dam failures: The environment tragedy of the largest technological disaster of Brazilian mining in global context." *Perspect. Ecol. Conserv.* 15 (3): 145–151. https://doi.org/10.1016/j.pecon.2017.06.002.

Fischer, H. B., E. J. List, R. C. Y. Koh, J. Imberger, and N. H. Brooks. 1979. *Mixing in inland and coastal waters*. New York: Academic Press.

IBAMA. 2016. "IBAMA—Instituto Brasileiro do Meio Ambiente e dos Recursos Naturais Renováveis." Accessed January 30, 2017. http://www.ibama.gov.br/phocadownload/emergenciasambientais/respostas_deliberacao_3_e_4_do_cif.pdf.

ICOLD (International Commission on Large Dams). 2001. *Tailings dams risk of dangerous occurrences, lessons learnt from practical experiences.* Bulletin 121. Paris: International Commission on Large Dams Committee on Tailings Dams and Waste Lagoons.

Jeyapalan, J. K., J. M. Duncan, and H. B. Seed. 1983. "Investigation of flow failures of tailings dams." *J. Geotech. Eng.* 109 (2): 172–189. https://doi.org/10.1061/(ASCE)0733-9410(1983)109:2(172).

Jin, M., and D. L. Fread. 1999. "1D modeling of mud/debris unsteady flows." *J. Hydraul. Eng.* 125 (8): 827–834. https://doi.org/10.1061/(ASCE)0733-9429(1999)125:8(827).

Julien, P. Y. 2010. *Erosion and sedimentation*. Cambridge, UK: Cambridge University Press.

Julien, P. Y. 2018. *River mechanics*. Cambridge, UK: Cambridge University Press.

Kashefipour, S. M., and R. A. Falconer. 2002. "Longitudinal dispersion coefficients in natural channels." *Water Res.* 36 (6): 1596–1608. https://doi.org/10.1016/S0043-1354(01)00351-7.

Kossoff, D., W. E. Dubbin, M. Alfredsson, S. J. Edwards, M. G. Macklin, and K. A. Hudson-Edwards. 2014. "Mine tailings dams: Characteristics, failure, environmental impacts, and remediation." *Appl. Geochem.* 51: 229–245. https://doi.org/10.1016/j.apgeochem.2014.09.010.

Kunkel, J. 2011. *Downstream modeling of tailings flow from failure of a 380-ft high tailing dam.* Denver: United States Society on Dams.

Lin, J., and J. Li. 2012. "Tailings dam break flow and sediment numerical simulation." *Civil Engineering and Urban Planning 2012 Proc.*, 677–683. Reston, VA: ASCE.

Marsooli, R., M. McGrath, and M. Altinakar. 2013. *2-D numerical modeling of tailings dam failure.* Oxford, MS: Univ. of Mississippi.

Marta-Almeida, M., R. Mendes, F. N. Amorim, M. Cirano, and J. M. Dias. 2016. "Fundão Dam collapse: Oceanic dispersion of River Doce after the greatest Brazilian environmental accident." *Mar. Pollut. Bull.* 112 (1): 359–364. https://doi.org/10.1016/j.marpolbul.2016.07.039.

McQuivey, R. S., and T. N. Keefer. 1974. "Simple method for predicting dispersion in streams." *J. Environ. Eng. Div.* 100 (4): 997–1011.

Morgenstern, N. R., S. G. Vick, C. B. Viotti, and B. D. Watts. 2016. *Report on the Immediate Causes of the Failure of the Fundão Dam.* São Paulo, Brazil: Cleary Gottlieb Steen & Hamilton LLP.

O'Brien, J. S., P. Y. Julien, and W. T. Fullerton. 1993. "Two-dimensional water flood and mudflow simulation." *J. Hydraul. Eng.* 119 (2): 244–261. https://doi.org/10.1061/(ASCE)0733-9429(1993)119:2(244).

ONS (Operador Nacional do Sistema Elétrico). 2017. "Operador Nacional do Sistema Elétrico." Accessed April 12, 2016. http://ons.org.br/Paginas/resultados-da-operacao/historico-da-operacao/dados_hidrologicos_vazoes.aspx.

Press, W. H., S. A. Teukolsky, W. T. Vetterling, and B. P. Flannery. 2007. *Numerical recipes: Art of scientific computing*. 3rd ed. Cambridge, UK: Cambridge University Press.

Rickenmann, D., D. Laigle, B. W. McArdell, and J. Hübl. 2006. "Comparison of 2D debris-flow simulation models with field events." *Comput. Geosci.* 10 (2): 241–264. https://doi.org/10.1007/s10596-005-9021-3.

Rico, M., G. Benito, and A. Díez-Herrero. 2008. "Floods from tailings dam failures." *J. Hazard. Mater.* 154 (1–3): 79–87. https://doi.org/10.1016/j.jhazmat.2007.09.110.

Rutherford, J. C. 1994. *River mixing*. New York: Wiley.

Schamber, D., and R. MacArthur. 1985. "One dimensional model for mud flows." In *Proc., ASCE Hydraulic Division Specialty Conf. on Hydraulics and Hydrology in the Small Computer Age*, 1–14. Orlando, FL: USACE.

Seo, I. W., and T. S. Cheong. 1998. "Predicting longitudinal dispersion coefficient in natural streams." *J. Hydraul. Eng.* 124 (1): 25–32. https://doi.org/10.1061/(ASCE)0733-9429(1998)124:1(25).

Tayfur, G., and V. P. Singh. 2005. "Predicting longitudinal dispersion coefficient in natural streams by artificial neural network." *J. Hydraul. Eng.* 131 (11): 991–1000. https://doi.org/10.1061/(ASCE)0733-9429(2005)131:11(991).

USBR (United States Bureau of Reclamation). 2015. *Technical evaluation of the gold king mine incident*, 132. Denver: USBR.

WISE (World Information Service on Energy Uranium Project). 2016. "Chronology of major tailings dam failures." Accessed May 26, 2017. http://www.wise-uranium.org/mdaf.html.

Zeng, Y., and W. Huai. 2014. "Estimation of longitudinal dispersion coefficient in rivers." *J. Hydro-Environ. Res.* 8 (1): 2–8. https://doi.org/10.1016/j.jher.2013.02.005.